ChemComm

Accepted Manuscript

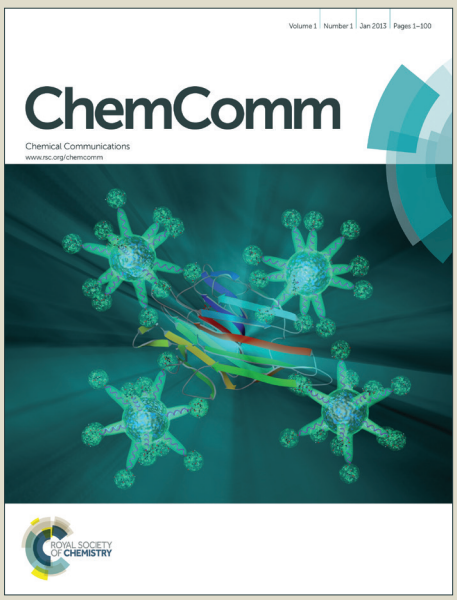

ROYAL SOCIETY OF CHEMISTRY

www.rsc.org/chemcomm

Cite this: DOI: 10.1039/c0xx00000x

www.rsc.org/xxxxxx

ARTICLE TYPE

High CO_2/N_2 and CO_2/CH_4 selectivity in a chiral metal-organic framework with contracted pores and multiply functionalities

Xiaoxia Lv,[‡] Liangjun Li,*[,§] Sifu Tang,[‡] Chao Wang,[‡] Xuebo Zhao*[,‡]

Received (in XXX, XXX) Xth XXXXXXXXX 20XX, Accepted Xth XXXXXXXXX 20XX

DOI: 10.1039/b000000x

A metal-organic framework with chiral pores and decorated imidazole and methyl groups was constructed. Upon activation, this MOF undergo a pore contraction and shows very high selectivity for CO_2/N_2 and CO_2/CH_4, indicating a synergistic effect of dynamic pores and functional groups.

Selective capture of CO_2 from flue gas and natural gas has become the most urgent issues driven by the concerns of climate change and demands in natural gas upgrading.[1] As an emerging type of crystalline porous materials, metal-organic frameworks (MOFs) have been proven the very promising materials for selective capture of CO_2 due to their high surface area and tuneable pore environments.[2] To achieve better selectivity, current efforts have been devoted to increasing the binding energy of gas molecules with frameworks by introducing high density of open metal sites[3] or by anchoring Lewis basic sites.[4] Moreover, theoretical and experimental studies revealed that CO_2 selectivity in MOFs could also be enhanced by introducing functional groups, such as methyl[5] or hydroxyl groups[6] by increasing the field potential of pores. While the conventional strategies are focusing on tuning the pore surface with homogeneous functional groups, anchoring mixed or multiply functional groups in a single MOF would also be intriguing.[7] These groups could function cooperatively when assembled in a single MOF which could have some benefits in improving the CO_2 selectivity.

Recently, a type of MOFs with flexible networks has attracted extensive interests due to their framework expansion or contraction triggered by external stimulus.[8] The intriguing properties of responding distinctly to different guest molecules make them very attractive in the fields of molecular recognition and selective gas sorption. MIL-53 is the most famous MOF that exhibits dynamic behaviours to CO_2 and water molecules.[9] C. J. Sumby et al. synthesized a MOF with ultrahigh CO_2/N_2 selectivity induced by the contraction of the rhombus pores.[10] Based on these materials, the contributions of structural transition to gas sorption selectivity were elucidated. However, the combinational effect of pore contraction/expansion and multiply functionalities on CO_2 selectivity, to the best of our knowledge, has not been reported yet. It is expected to be able to further enhance the selectivity of CO_2 under the synergism of these factors.

In this paper, a new MOF (compound **1**) with incorporated imidazole and methyl functional groups in 1D rectangle channels was synthesized by using a rigid imidazole-carboxylate ligand: 4,4'-(5,6-dimethyl-1H-benzo[d]imidazole-4,7-diyl)-dibenzoic acid (**H_3L**) and Zn(II) ions. Upon activation, a structural transition has occurred and a new structure with contracted pores was generated due to high flexibility of coordination spheres.[11] Subsequent to structural characterization, the single-component gas sorption properties and ultrahigh gas selectivities towards CO_2/N_2 and CO_2/CH_4 on the activated sample were studied.

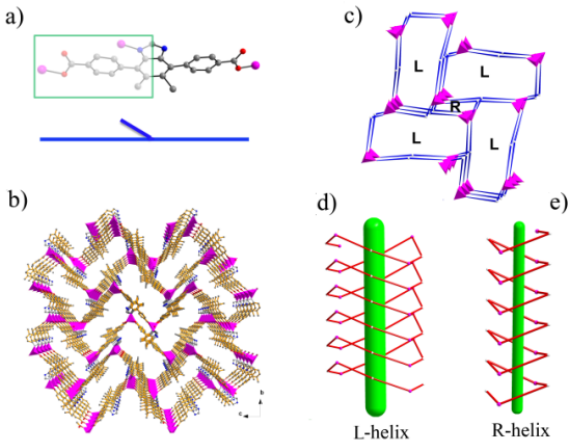

Fig. 1 (a) Presentation of coordination modes and simplified structure of ligand; (b) The channels in **1** viewing from *a* axis; (c) The topological network of **1**; (d) Simplified structure of the L-helix channel; (e) Simplified structure of the R-helix chain.

Colorless columnar crystals of $[Zn(L)\cdot H_2O]\cdot DMA$ (**1**) was obtained via solvothermal reaction of **H_3L** and $Zn(NO_3)_2\cdot 6H_2O$ in DMA/H_2O (1/1) solution at 100 °C for 48 hours (see experimental details in †ESI, S1). Single crystal X-ray analysis

§ *Institute of Unconventional Hydrocarbon and New Energy Sources, China University of Petroleum (East China), Qingdao 266580, China*
E-mail: liliangjun1982@hotmail.com
‡ *Qingdao Institute of Bioenergy and Bioprocess Technology, Chinese Academy of Sciences, Qingdao 266101, China*
Fax: +86 0532-80662728; E-mail: zhaoxb@qibebt.ac.cn

† Electronic Supplementary Information (ESI) available: Experimental details, crystallographic data, structure representation, IR and TGA diagrams, calculation details about Q_{st} and IAST selectivity are provided. CCDC 963443. See DOI: 10.1039/b000000x/

reveals that **1** crystallizes in the chiral orthorhombic space group $P2_12_12_1$. The carboxylate groups in this ligand are coordinated by two Zn(II) ions in a monodentate form, while one of the nitrogen atoms in imidazole moiety is deprotonated and coordinated by another Zn(II) atom. The self-assembly of ligands with the tetrahedrally coordinated Zn(II) ions finally gives a three-dimensional network, with a series of parallel one-dimensional rectangle channels (1.1×2.1 nm) running along *a* axis (as shown in Fig. 1b). The methyl groups and the uncoordinated imidazole nitrogen atoms are fully exposed in the pores, ensuring their interactions with gas molecules during sorption. By simplifying ligands and metal centres into a T-shaped linkers and three-connected nodes, the structure of **1** can be viewed as a network composed of the smaller R-helix rectangular chain surrounded with four larger L-helix channels as shown in Fig.1c. The combination of the L-helix channels and R-helix chains give rise to a network with a rare $SrSi_2$ topology.[12] Finally, the 1D rectangular channels with L-helix homochirality are observed when considering the Van-der Waal radis. The guest accessible volume of **1** is 45.2% calculated from crystallographic data.

The good match between Powder X-ray diffraction (PXRD) patterns of as-synthesized sample and simulated pattern from crystallographic data confirms the iso-structure and purity of bulk sample (as shown in †ESI, Fig. S7). In order to fully activate the sample, the as-synthesized MOF was solvent exchanged with acetone in a Soxhlet-extractor for 48 h, followed by heating at 353 K for 12 h under ultrahigh vacuum (10^{-7} mbar). The shift of peaks in PXRD pattern of the activated sample indicates that the framework of this MOF have undergone a structural transition from its original structure to a new phase (termed as **1a**). However, this kind of transition is reversible, as indicated by the structural transition from **1a** to the original phase of **1** when soaking the activated MOF in DMA/H_2O (1/1, v/v) solution for 24 hours. After several cycles of adsorption and desorption, the structure and crystallinity of this MOF remain unchanged. Further, the structure of this MOF retains well when exposing the activated MOF to moisture or soaking the activated MOF in water for 24 hours, suggesting good structural stability and water stability of this MOF (see PXRD patterns in †ESI, Fig. S8).

To investigate the gas sorption properties of **1a**, N_2, CO_2 and CH_4 sorption measurements were conducted on an Intelligent Gravimetric Analyzer (IGA-001). As shown in Fig. S9, it shows nearly no uptakes for N_2 at 77 K, but it adsorbs a significant amount of N_2 at 195 K (3.5 wt%) and 273 K (1.5 wt%) (see Fig. 2a). These results indicate that the as-synthesized sample has undergone a contraction upon the solvent exchange and evacuation. The pore size of **1a** may be close to the kinetic diameter of N_2 (3.64 Å),[13] and the large diffusional resistances led to the non-adsorption of N_2 at 77 K. However, at higher temperatures (195 K or room temperatures), the diffusion resistance could be overcome due to additional thermal energy of N_2 molecules. At 195 K, N_2 adsorption shows a three-step process: subsequent to a very obscure adsorption at low pressure (0~0.26 bar), a steep increase is observed on the isotherm, followed by another significant increase in N_2 uptake at 10 bar, and finally a N_2 uptake of 3.5 wt% is reached. The desorption branch does not trace the adsorption isotherm and therefore led to a large hysteric loop. The stepwise and hysteric N_2 isotherm indicates the pore expansion when N_2 molecules getting into the pores of **1a** at 195 K. Interestingly, at 273 K the adsorption-desorption curves are reversible with virtually no hysteresis and the uptake of N_2 is decreased compared to 195 K due to thermodynamic reasons.

CO_2 isotherms at 195 K (Fig. S9) and room temperatures (Fig. 2b) show smooth and hysteric type-I isotherms, with the degree of hysteresis decreasing with increasing temperatures. The smooth and hysteric isotherm for CO_2 is rare in literature, and it may be attributed to the small pore windows and pore expansion in this MOF, which is also observed in [Cu(bcppm)H_2O]-*ac*.[10] At higher temperatures, the thermal vibrations of the framework and gas molecules are intensified and lead to the weaker potential of molecular retention, and thus give the smaller hysteric loops in CO_2 isotherms at higher temperatures. The adsorption capacity of CO_2 on **1a** is 0.93 mmol g^{-1} at 273 K and 1 bar, which is relatively low compared to those MOFs with high adsorption capacities,[14] but is consistent with the limited surface area observed in **1a**. Using the CO_2 isotherm at 273 K in the pressure range of 0~20 bar, the pore volume and pore width of the **1a** can be determined as 0.0558 $cm^3 \cdot g^{-1}$ and 0.42 nm, respectively, based on the Dubinin-Radushkevich (DR) analysis[15] (see details in †ESI, S4). The values of pore volume and pore width of **1a** are largely reduced compared to the as-synthesized MOF, supporting the conclusion that the pores of this MOF has contracted upon activation. CH_4 isotherm measured at room temperature shows the similar isotherms as CO_2 except for the lower uptakes and less obvious hysteric loops (as shown in †ESI, S4), indicating the weaker interactions of CH_4 molecules with the framework.

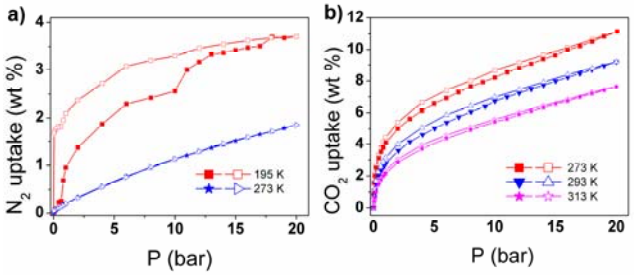

Fig. 2 Isotherms at different temperatures for (a) N_2 and (b) CO_2 (solid symbols: adsorption; hollow symbols: desorption.)

The abundant imidazole and methyl groups pending in the pores and the difference in structural response towards CO_2, CH_4 and N_2 encouraged us to investigate the CO_2 selectivity over CH_4 and N_2. To predict CO_2/CH_4 and CO_2/N_2 binary mixture selectivity, the ideal adsorbed solution theory (IAST) calculation coupled with a dual-site Langmuir-Freundlich simulation was employed on the basis of single-component isotherms (see details in †ESI, S5). It has been verified by many studies that the IAST model can predict gas mixture adsorption accurately on many zeolites and MOF materials.[16] Fig. 3a shows the predicated selectivities for CO_2/CH_4 and CO_2/N_2 as the function of pressure when gas phase mole fraction are 5/95 and 15/85 which are typical feed compositions for natural gas and flue gas, respectively. It is worth noticing that very high selectivities for both of the CO_2/CH_4 and CO_2/N_2 are obtained. The maximum values of selectivities for CO_2/CH_4 and CO_2/N_2 are 513 and 867 at low pressure (0.1 bar), respectively. At 1 bar, the corresponding values are 151 and 252, respectively, which are

significantly higher than those MOFs with homogenous amine[17] or methyl functional group[18] and are comparable to the MOFs with highest selectivity reported in literatures.[6a, 16b] When the pressure is increasing, the selectivities are decreasing. When the pressure is 20 bar, the selectivities for CO_2/CH_4 and CO_2/N_2 are 30 and 51, respectively. These results suggest that **1a** have very high selectivity for CO_2/CH_4 and CO_2/N_2 and could be an excellent candidate for the selective sorption of CO_2 from natural gas and flue gas under variable working conditions.

Moreover, the CO_2/CH_4 and CO_2/N_2 selectivities as the function of feed composition at 1 bar and 273 K were investigated (as shown in Fig. 3b). Both of CO_2/CH_4 and CO_2/N_2 selectivities increase significantly with the increasing gas phase mole fraction of CH_4 and N_2. In the case of y_{CH4}= 0.5, the selectivity of CO_2/CH_4 is 52. As for CO_2/N_2, the selectivity of CO_2/N_2 is 134 at 1 bar when y_{N2} = 0.5. These values are lying in top ranks of selectivities for CO_2/CH_4 and CO_2/N_2 in MOF materials.[19] To investigate separation performance of this MOF on real CO_2/CH_4 and CO_2/N_2 gas mixtures, the gravimetric sorption experiment, a technique established by Van Ness[20] and validated by many gas separation experiments,[21] was employed for the analysis of CO_2/CH_4 and CO_2/N_2 adsorption separation on **1a**. As shown in Fig. 3c and 3d, the experimental mixed gas isotherms for CO_2/CH_4 (y_{CO2}=0.429) and CO_2/N_2 (y_{CO2}=0.433) gas mixtures are consistent well with the mixed gas isotherms predicated by IAST calculations at the same feed compositions and separation conditions (as shown in Fig. 3c and 3d), indicating the good reliability of the results of IAST calculations and the high CO_2/CH_4 and CO_2/N_2 selectivity of this MOF. The minor differences between experimental and predicated isotherms could be attributed to the non-ideality of gas mixtures deviating from ideal solution.

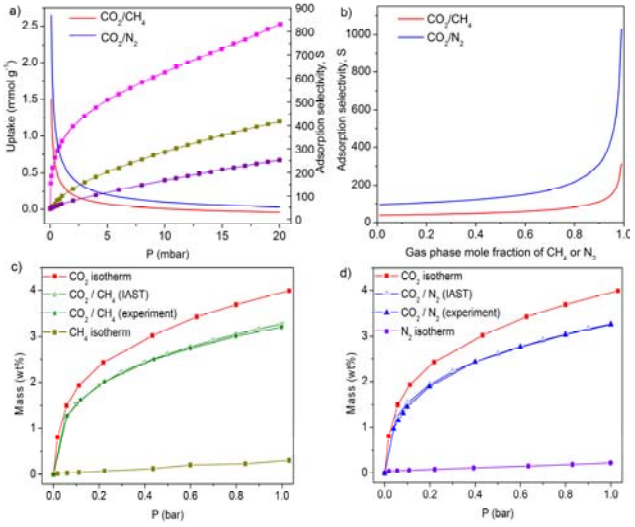

Fig. 3 (a) Selectivities of CO_2 over CH_4 and N_2 predicted by IAST at 273 K. (b) Selectivities of CO_2 over CH_4 and N_2 as the function of gas phase compositions at 1 bar and 273 K predicated by IAST. (c) Comparison between the mixed gas isotherms predicated by IAST (hollow) (y_{CO2}=0.429) and experimental mixed gas isotherms (solid) (y_{CO2}=0.429) for CO_2/CH_4. (d) Comparison between the mixed gas isotherms predicated by IAST (hollow) (y_{CO2}=0.433) and experimental mixed gas isotherms (solid) for CO_2/N_2 (y_{CO2}=0.433).

The high values of CO_2 selectivity over CH_4 and N_2 could be rationalized by the high adsorption enthalpy (Q_{st}) for CO_2 but moderate values for CH_4 on **1a** (see Q_{st} plots in †ESI, S6). The Q_{st} at zero surface coverage ($Q_{st(n=0)}$) for CO_2 is 43.7±3.1 kJ mol^{-1} which is higher than many common MOFs and similar to those MOFs with Lewis basic groups or open metal sites[3b, 19], indicating the strong interaction strength of CO_2 molecules with the framework. In contrast, CH_4 shows much weaker interaction strength with the framework, with a $Q_{st(n=0)}$ value of 16.4 ±1.3 kJ mol^{-1} which is within the normal range of Q_{st} of CH_4 adsorption on porous materials[22]. The combinational effects of imidazole and methyl functional groups coupled with specific confined pores in **1a** may attribute to the large initial interaction strength of CO_2 with the frameworks, but these factors have much less effect on CH_4 or N_2 molecules due to their nonpolar moments. Therefore, the synergistic effects of both surface chemistry and different structural transitions for different gas molecules could account for the very high selectivities for CO_2/CH_4 and CO_2/N_2 at low pressures. At higher pressures, the Q_{st} of CO_2 gradually decreases with increasing loading, indicating the preferable adsorption sites being occupied gradually. However, the gas selectivities for CO_2/CH_4 and CO_2/N_2 lie in range of 30~151 and 51~252, respectively, which are still very high values of selectivity in MOFs.

In summary, a 3D MOF with 1D rectangular chiral channels decorated with imidazole and methyl functional groups was synthesized. PXRD patterns combined with gas adsorptions confirm the pore contraction and the following pore expansion when accommodating guest molecules. The different extent of hysteresis in isotherms of CO_2, CH_4 and N_2 indicate the different response of framework towards different guest molecules. The synergistic effects of imidazole and methyl functional groups coupled with contracted pores enable this MOF with very high selectivity for CO_2/CH_4 and CO_2/N_2, suggesting a promising candidate for selective CO_2 capture from flue gas and purification of natural gas.

This work was supported by grants from the National Natural Science Foundation of China (NSFC) (grant No. 21073216 and 21173246) and the "Hundred-Talent Project" (KJCX2-YW-W34) of the Chinese Academy of Sciences.

Notes and references

1 a) J. R. Li, J. Sculley and H. C. Zhou, *Chem. Rev.*, 2012, **112**, 869; b) S. Xiang, Y. He, Z. Zhang, H. Wu, W. Zhou, R. Krishna and B. Chen, *Nat Commun*, 2012, **3**, 954.

2 a) J. Liu, P. K. Thallapally, B. P. McGrail, D. R. Brown and J. Liu, *Chem. Soc. Rev.*, 2012, **41**, 2308-2322; b) P. K. Thallapally, R. K. Motkuri, C. A. Fernandez, B. P. McGrail and G. S. Behrooz, *Inorg. Chem.*, 2010, **49**, 4909-4915;

3 a) S. R. Caskey, A. G. Wong-Foy and A. J. Matzger, *J. Am. Chem. Soc.*, 2008, **130**, 10870-10871; b) D. Britt, H. Furukawa, B. Wang, T. G. Glover and O. M. Yaghi, *P. Natl. Acad. Sci.*, 2009, **106**, 20637-20640.

4 a) X. Si, C. Jiao, F. Li, J. Zhang, S. Wang, S. Liu, Z. Li, L. Sun, F. Xu, Z. Gabelica and C. Schick, *Energ. Environ. Sci.*, 2011, **4**, 4522-4527; b) L. Li, S. Tang, C. Wang, X. Lv, M. Jiang, H. Wu and X. Zhao, *Chem.Commun.*, 2013, **50**, 2304-2307.

5 a) H. Liu, Y. Zhao, Z. Zhang, N. Nijem, Y. J. Chabal, H. Zeng and J. Li, *Adv. Funct. Mater.*, 2011, **21**, 4754-4762; b) Y. T. Huang, W. P. Qin, Z. Li and Y. W. Li, *Dalton Trans.*, 2012, **41**, 9283-9285.

6 a) H.-L. Jiang, D. Feng, T.-F. Liu, J.-R. Li and H.-C. Zhou, *J. Am. Chem. Soc.*, 2012, **134**, 14690-14693; b) Z. X. Chen, S. C. Xiang, H. D. Arman, J. U. Monda, P. Li, D. Y. Zhao and B. L. Chen, *Inorg. Chem.*, 2011, **50**, 3442-3446; c) Z. X. Chen, S. C. Xiang, H. D. Arman, P. Li, D. Y. Zhao and B. L. Chen, *Eur. J. Inorg. Chem.*, 2011, 2227-2231.

7 X. Kong, H. Deng, F. Yan, J. Kim, J. A. Swisher, B. Smit, O. M. Yaghi and J. A. Reimer, *Science*, 2013, **341**, 882-885.
8 a) Y. Sakata, S. Furukawa, M. Kondo, K. Hirai, N. Horike, Y. Takashima, H. Uehara, N. Louvain, M. Meilikhov, T. Tsuruoka, S. Isoda, W. Kosaka, O. Sakata and S. Kitagawa, *Science*, 2013, **339**, 193-196; b) S. Yang, L. Liu, J. Sun, K. M. Thomas, A. J. Davies, M. W. George, A. J. Blake, A. H. Hill, A. N. Fitch, C. C. Tang and M. Schröder, *J. Am. Chem. Soc.*, 2013, **135**, 4954-4957; c) P. K. Thallapally, J. Tian, M. Radha Kishan, C. A. Fernandez, S. J. Dalgarno, P. B. McGrail, J. E. Warren and J. L. Atwood, *J. Am. Chem. Soc.*, 2008, **130**, 16842-16843.
9 S. Bourrelly, P. L. Llewellyn, C. Serre, F. Millange, T. Loiseau and G. Férey, *J. Am. Chem. Soc.*, 2005, **127**, 13519-13521.
10 W. M. Bloch, R. Babarao, M. R. Hill, C. J. Doonan and C. J. Sumby, *J. Am. Chem. Soc.*, 2013, **135**, 10441-10448.
11 C. A. Fernandez, P. K. Thallapally, R. K. Motkuri, S. K. Nune, J. C. Sumrak, J. Tian and J. Liu, *Cryst. Growth Des.*, 2010, **10**, 1037-1039.
12 Y.-G. Huang, B. Mu, P. M. Schoenecker, C. G. Carson, J. R. Karra, Y. Cai and K. S. Walton, *Angew. Chem. Int. Ed.*, 2011, **50**, 436-440.
13 Y.-S. Bae, O. K. Farha, J. T. Hupp and R. Q. Snurr, *J. Mater. Chem.*, 2009, **19**, 2131-2134.
14 a) P. L. Llewellyn, S. Bourrelly, C. Serre, A. Vimont, M. Daturi, L. Hamon, G. De Weireld, J.-S. Chang, D.-Y. Hong, Y. Kyu Hwang, S. Hwa Jhung and G. r. Férey, *Langmuir*, 2008, **24**, 7245-7250; b) L. Li, S. Tang, X. Lv, M. Jiang, C. Wang and X. Zhao, *New J. Chem.*, 2013, **37**, 3662-3670.
15 a) J. Garrido, A. Linares-Solano, J. M. Martin-Martinez, M. Molina-Sabio, F. Rodriguez-Reinoso and R. Torregrosa, *Langmuir*, 1987, **3**, 76-81; b) D. Cazorla-Amorós, J. Alcañiz-Monge and A. Linares-Solano, *Langmuir*, 1996, **12**, 2820-2824; c) D. Lozano-Castelló, D. Cazorla-Amorós and A. Linares-Solano, *Carbon*, 2004, **42**, 1233-1242.
16 a) Y.-S. Bae, K. L. Mulfort, H. Frost, P. Ryan, S. Punnathanam, L. J. Broadbelt, J. T. Hupp and R. Q. Snurr, *Langmuir*, 2008, **24**, 8592-8598; b) P. Nugent, Y. Belmabkhout, S. D. Burd, A. J. Cairns, R. Luebke, K. Forrest, T. Pham, S. Ma, B. Space, L. Wojtas, M. Eddaoudi and M. J. Zaworotko, *Nature*, 2013, **495**, 80-84.
17 J. Duan, Z. Yang, J. Bai, B. Zheng, Y. Li and S. Li, *Chem.Commun.*, 2012, **48**, 3058-3060.
18 H. Jasuja and K. S. Walton, *J. Phys. Chem. C*, 2013, **117**, 7062-7068.
19 K. Sumida, D. L. Rogow, J. A. Mason, T. M. McDonald, E. D. Bloch, Z. R. Herm, T.-H. Bae and J. R. Long, *Chem. Rev.*, 2012, **112**, 724-781.
20 H. C. Van Ness, *Ind. Eng. Chem. Fundamen.*, 1969, **8**, 464-473.
21 a) A. L. Myers, C. Minka and D. Y. Ou, *AIChE J.*, 1982, **28**, 97-102; b) F. Karavias and A. L. Myers, *Chem. Eng. Sci.*, 1992, **47**, 1441-1451; c) R. Van Der Vaart, C. Huiskes, H. Bosch and T. Reith, *Adsorption*, 2000, **6**, 311-323; d) L. Hamon, E. Jolimaître and G. D. Pirngruber, *Ind. Eng. Chem. Res.*, 2010, **49**, 7497-7503.
22 T. A. Makal, J.-R. Li, W. Lu and H.-C. Zhou, *Chem. Soc. Rev.*, 2012, **41**, 7761-7779.